An MHD Study of the Behavior of an Electrolyte Solution using3D Numerical Simulation and Experimental results

Luciano Pires Aoki*[1], Harry Edmar Schulz[1], Michael George Maunsell[1]
[1]University of São Paulo – School of Engineering at São Carlos, São Paulo, Brazil
*Corresponding author: Av. Trabalhador São Carlense 400 (São Carlos, S.P.), Brazil, 13566-590
lucianoaoki@gmail.com

Abstract: This article considers a closed water circuit with square cross section filled with an electrolyte fluid. The conductor fluid was moved using a so called electromagnetic pump, or EMP, in which a permanent magnet generates a magnetic field and electrodes generate the electric field in the flow. Thus, the movement is a consequence of the magnetohydrodynamic (or MHD) effect. The model adopted here was derived from the Navier-Stokes equations for Newtonian incompressible fluid using the k-ε turbulence model and coupled with the Maxwell equations. The equations were solved using COMSOL Multiphysics® version 3.5a (2008). The 3D numerical simulations allowed obtaining realistic predictions of the Lorentz forces, the current densities, and the movement of the flows as a consequence of the MHD effects, imposing direct currents.

Keywords: electromagnetic pump, magnetohydrodynamic, MHD simulations, MHD experiments, Lorentz force.

1. Introduction

Magnetohydrodynamics or simply (MHD) is the field of science that studies the movement of conductive fluids subjected to electromagnetic forces. This phenomenon brings together concepts of fluid dynamics and electromagnetism. Formally, MHD is concerned with the mutual interactions between fluid flows and magnetic fields. Electrically conducting and non-magnetic fluids must be used, which limits the applications to liquid metals, hot ionized gases (plasmas) and electrolytes. Over the years, MHD has been applied to a wide spectrum of technological devices, directed, for example, to electromagnetic propulsion or to biological studies.

Ritchie (1832) [1] was probably the first that gave the needed attention to the MHD phenomenon. He described the basic principles of an MHD pump, where an electric current and a magnetic field pass through an electrolyte solution.

The electromagnetic pumping (EMP) of an electrically conductive fluid described in the present study uses a direct current (DC) MHD device. Williams [2] described this concept in 1930, applying it to pump liquid metals in a channel. In the DC EMP used in this study, a direct current was applied across a rectangular section of the closed channel filled with salt water, and submitted to a non-uniform magnetic field perpendicular to the current. The interactions between current and magnetic fields produced electromagnetic forces or Lorentz forces, driving the fluid through the channel. The EMP is of growing interest in many industrial applications, requiring precise flow controls, enabling to induce flow deviations without mechanical moving parts or devices [3].

1.1 MHD investigations in the literature

There are many studies in the literature directed to the description of velocity profiles and MHD parameters. The study of Andreev et al. (2006) [4] may be cited as an example, showing an experimental study for a conductor liquid metal under the influence of a non-homogeneous magnetic field. Unlike a macropump, the arrangement acts like a flow brake, and it is applicable in mining industries.

As a second example, Ramos and Winovich (1990) [5] applied the finite element method to simulate a MHD channel flow as a function of the Reynolds number and the wall conductivity. Finally, as a last example for the present study, Lemoff and Lee (2000) [6] applied a computational method to describe a micro fluidic pump using alternating current (AC) MHD propulsion to move the electrolyte solution.

In the present study an experimental device was built to obtain data for movement of salty water. Numerical simulations were then performed to calibrate the code and to allow predicting the flow situations. This paper describes the performed numerical simulations.

2. Theoretical analysis

The formulation of the MHD steady state model was derived from Maxwell equations coupled with Navier-Stokes equations. Therefore the phenomena are described by the electromagnetism and the fluid dynamics equations. From the electromagnetism equations it follows that:

$$\nabla \cdot \mathbf{E} = \frac{\rho_e}{\varepsilon_0} \quad \text{(Gauss law)} \qquad (1)$$

$$\nabla \times \mathbf{E} = -\frac{\partial \mathbf{B}}{\partial t} \quad \text{(Faraday law)} \qquad (2)$$

$$\nabla \cdot \mathbf{B} = 0 \quad \text{(No magnetic monopoles)} \qquad (3)$$

$$\nabla \times \mathbf{B} = \mu_0 \mathbf{J} + \mu_0 \varepsilon_0 \frac{\partial \mathbf{E}}{\partial t} \quad \text{(Ampère law)} \qquad (4)$$

Equations (1), (2), (3) and (4) represent the Maxwell equations. Using the divergence theorem and applying the Gauss Law it follows that:

$$\nabla \cdot \mathbf{J} = -\varepsilon_0 \frac{\partial}{\partial t} \nabla \cdot \mathbf{E} = -\frac{\partial \rho_e}{\partial t} \text{ or } \nabla \cdot \mathbf{J} = 0 \qquad (5)$$

In MHD problems, the second term, $\frac{\partial \rho_e}{\partial t}$, is negligible for a conductor. The Ohm´s Law and the Ampère´s Law conduce to:

$$\nabla \times \left(\frac{\nabla \times \mathbf{A}}{\mu_0} \right) = \mathbf{J} \text{ or } \nabla \times \mathbf{B} = \mu_0 \mathbf{J} \qquad (6)$$

$$\mathbf{J} = \sigma \left[-\nabla \phi + \mathbf{u} \times (\nabla \times \mathbf{A}) \right] \qquad (7)$$

Equation (7) is a convenient form of the Ohm's Law. Equations (5) and (6) represent, respectively, the conservation of the electrical current and the so called Maxwell-Ampère Law. In equation (7), $\mathbf{J}$ is the total current density, σ is the electrical conductivity of the fluid, ϕ is the electric potential, $\mathbf{u}$ is the fluid velocity and $\mathbf{A}$ is the magnetic vector potential. Notice that $\mathbf{B} = (\nabla \times \mathbf{A})$ and $\mathbf{E} = -\nabla \phi$.

From the fluid dynamics and the k-ε turbulence model, we have:

$$\nabla \cdot \mathbf{u} = 0 \qquad (8)$$

$$\rho (\mathbf{u} \cdot \nabla) \mathbf{u} = \nabla \cdot \left[-p\mathbf{I} + (\eta + \eta_T) \left(\nabla \mathbf{u} + (\nabla \mathbf{u})^T \right) \right] + \mathbf{F} \qquad (9)$$

$$\rho \mathbf{u} \cdot \nabla k = \nabla \cdot \left[\left(\eta + \frac{\eta_T}{\sigma_k} \right) \nabla k \right] + \eta_T P(\mathbf{u}) - \rho \varepsilon \qquad (10)$$

$$\rho \mathbf{u} \cdot \nabla \varepsilon = \nabla \cdot \left[\left(\eta + \frac{\eta_T}{\sigma_\varepsilon} \right) \nabla \varepsilon \right] + \frac{C_{\varepsilon 1} \varepsilon \eta_T P(\mathbf{u})}{k} - \frac{C_{\varepsilon 2} \rho \varepsilon^2}{k} \qquad (11)$$

Where:

$$P(\mathbf{u}) = \nabla \mathbf{u} : \left(\nabla \mathbf{u} + (\nabla \mathbf{u})^T \right) \qquad (12)$$

$$\eta_T = \rho C_\mu k^2 / \varepsilon \qquad (13)$$

Equations (8), (9), (10) and (11) represent respectively the conservation of mass, momentum, turbulence kinetic energy k and dissipation rate ε of the fluid in motion. C_μ, $C_{\varepsilon 1}$, $C_{\varepsilon 2}$, σ_k and σ_ε are constants. These equations are described in the COMSOL model library [7].

The coupling between the electromagnetic model and the fluid dynamics model is achieved by introducing the Lorentz force $\mathbf{F}$, given by $\mathbf{F} = (\mathbf{J} \times \mathbf{B})$, as a body force in the movement equations.

3. The MHD problem and the numerical modeling

As previously mentioned, the electromagnetic pump moved the salty water along the channel as a consequence of the orthogonal fields shown in figure 1, which are perpendicular to the movement of the fluid. A DC current was applied using aluminum electrodes while a non-uniform magnetic field was applied perpendicular to the current. The Lorentz force was generated through the interactions between these two fields. A sketch of the circuit and the formation of the Lorentz force can be seen in figure 1.

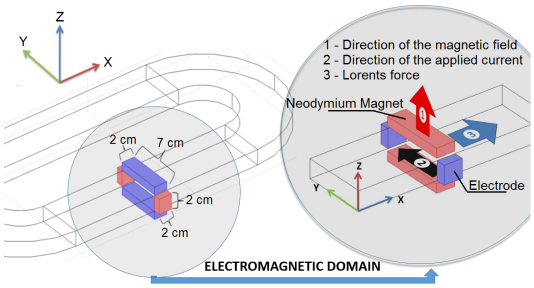

Figure 1. The MHD model and the closed circuit.

The dimensions of the electromagnetic domain (EMD), the electrodes and the magnets can be seen in figure 2. The bed of the channel is located at the horizontal *x,y* plane , that is, $z = 0$. For the simulations, the physical characteristics of the fluid, like density and dynamic viscosity, were adjusted to represent salty water. An external electrical field was applied along the circuit, simulating the real power supply.

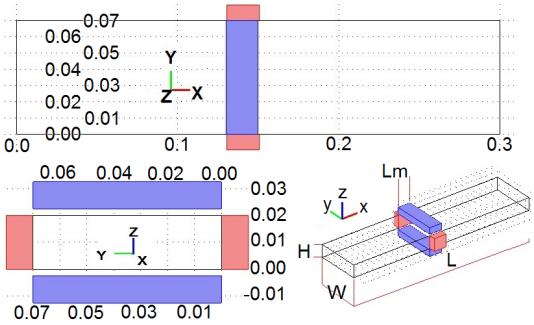

Figure 2. Channel with length L=0.3 m, height H=0.02 m and width W=0.07 m. The magnets have length Lm=0.02 m.

The EMD is bounded by an air sphere, representing the environmental conditions. Proper initial conditions were imposed to begin the simulations. The 3D MHD equations were solved using the finite element method furnished by the program COMSOL Multiphysics® 3.5a (2008), together with the with the k-ε turbulence model, the magnetostatics and conductive media of the DC models. The boundary conditions applied in the models inserted in code are presented in table 1.

Table 1: Parameters used in the simulations

Equation Type	Boundary Conditions
Electromagnetics	B(x ; y ; 0.03) = B_z (+) 0.13 < x < 0,15 ; 0 < y < 0,07 B(x ; y ; -0.13) = B_z (-) 0.13 < x < 0.15 ; 0 < y < 0.07 *Electrodes* ϕ (x ; 0.08 ; z) = V (+) 0.13 < x < 0,15 ; 0 < z < 0,02 ϕ (x ; -0.01 ; z) = V (-) 0.13 < x < 0.15 ; 0 < z < 0.02 *Insulations* Magnetically insulated elsewhere Electrically insulated elsewhere
Fluid Dynamics	U(x ; 0 ; z) = 0 (no-slip), U(x ; y ; 0) = 0 (no-slip) U(x ; 0.07 ; z) = 0 (no-slip), U(x ; y ; 0.02) = 0 (no-slip) *Inlet* U(0 ; y ; z) = 2 U_0 *U*1*s1*(1-s1)*s2*(1-s2) ; 0 < y < 0.07 ; 0 < z < 0.02 *Outlet* P(0.3 ; y ; z)=0 ; 0 < y < 0.07 ; 0 < z < 0.02 Body force = F_l = Lorentz force

The remanent flux density of the magnets was set as $\mathbf{B}_r$ = 1.21 T (neodymium magnets, grade N35) and the relative permeability of the entire system was set in μ_r = 1. The electrical conductivity of the air, the salty water and the electrodes was set as σ_{air} = 1E-14 S/m, σ_{water} = 5 S/m and $\sigma_{electrode}$ = 3.7E7 S/m, respectively. The density of the salty water was set as ρ_{water} = 1020 kg/m^3 and the dynamic viscosity was set as η_{water} = 1E-3 Pa.s.

The parameters U_0 and U represents the maximum and mean velocities respectively, and the arc length parameters s1 and s2 shown in table 1 create a 3D parabolic velocity profile at inflow boundaries.

The inlet velocity conditions are different at the left and right walls of the channel, because the observed velocities were faster in the outer part of the channel due to geometry effects (the two curves).

An iterative solving procedure was used. Firstly, the magnetic flux density **B** was solved. Then the electrical potential ϕ, the electric field **E**, and the current density **J** were determined by solving the Poisson and the Ohm´s Laws. In the

first iteration, the parcel corresponding to equation (7), $\mathbf{u}\times(\nabla\times\mathbf{A})$, is zero because the fluid is still in rest. The current density is calculated by $\mathbf{J} = -\sigma\nabla\phi$. After having calculated the Lorentz through the rotational of **B**, the resulting electromagnetic force was coupled with the Navier-Stokes equation (9), furnishing an initial value for the velocity of the flow.

In order to obtain different current densities, velocity profiles and Lorentz forces, two different cases were simulated for voltages of 12 V and 30 V across the electrodes. For the simulation a mesh of 108546 elements was adopted. It generates 554462 degrees of freedom.

4. Results and discussions

Different aspects of the electromagnetic pump were analyzed.

The magnetic flux density distribution along the electrodes (*y* direction) is shown in figure 3.

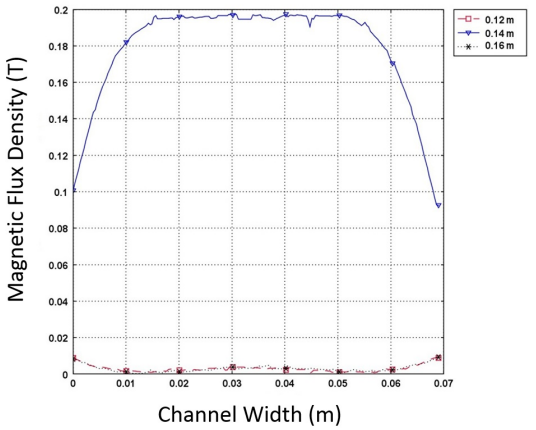

Figure 3. Magnetic flux density along the *y*-axis for different *x* positions.

The maximum value of the magnetic flux attained about 0.2 T and was located in the middle of the channel, while the value of the magnetic flux near the electrodes was of the order of 0.1 T. Note that for different *x* positions in the channel, the magnetic flux is nearly negligible (about 0.01 – 0.009 T).

Figure 4 shows the magnetic flux density along the *x*-axis direction. Again, the intensity of the magnetic field is stronger at the center of the electromagnetic domain (about 0.2 T).

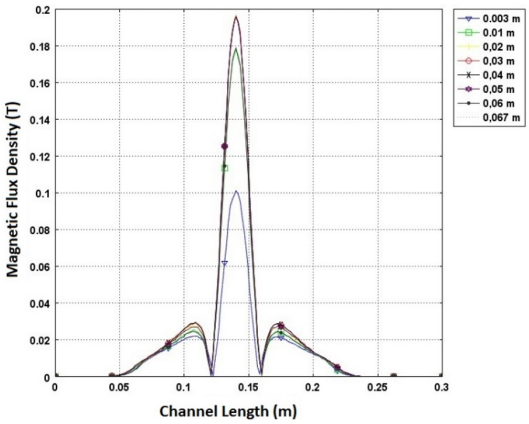

Figure 4. Magnetic flux density along the *x*-axis for different *y* positions.

The results of the two values of voltage studied here are presented in table 2.

Table 2: Results for the two voltages tested here

Case	Applied voltage (V)	Max. velocity (m/s)	Max. Lorentz force (N/m^3)
1	12	0.095	580
2	30	0.146	920

Figures 5 and 6 show the calculated Lorentz forces acting in the channel for the two voltages.

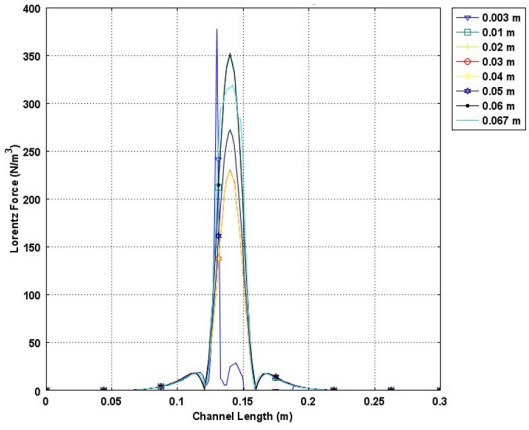

Figure 5. Lorentz force along the *x*-axis for different *y* positions and 12 Volts.

As expected, the electromagnetic forces were more intense in the middle of the channel and increased with the applied voltage.

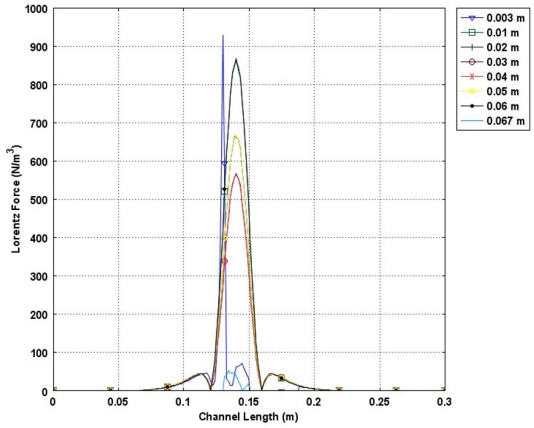

Figure 6. Lorentz force along the *x*-axis for different *y* positions and 30 Volts.

The Lorentz force was also calculated along the *y*-axis, between the electrodes. Figure 7 illustrates that, for three voltages tested in this case (12 V, 30 V, and, in this case, also 20 V) the Lorentz force showed to be stronger near the walls (the position of the electrodes) than in the middle of the channel.

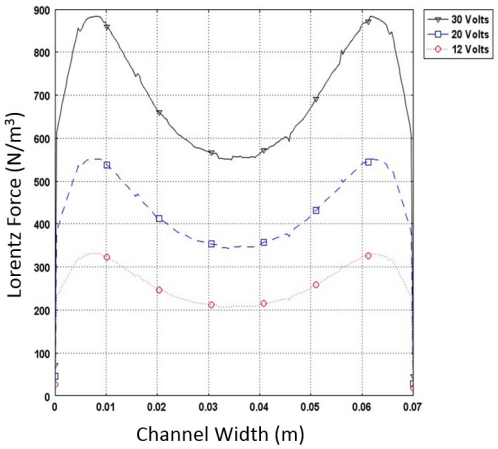

Figure 7. Lorentz forces along the *y*-axis for different voltages.

Figures 8 and 9 show the velocity profiles for different positions *x* along the channel, imposed by the Lorentz force distribution shown in figure 7.

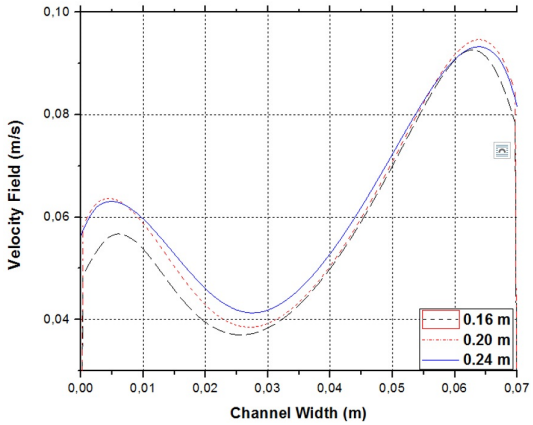

Figure 8. Fluid velocity profile along the *y*-axis for different *x* positions and 12 volts.

As expected from the distribution of the Lorentz force, the velocity profiles show higher velocity values near de walls, and lower values in the middle region. The asymmetry was imposed through the boundary conditions, and following the experimental observations. Nevertheless, the M-shape profile of figure 7 is reproduced by figures 8 and 9. Similar results were obtained by Kandev et all [8], where a molten metal was pumped along a flat channel subjected to electromagnetic forces, and by Andreev et all [4], where a liquid metal was subjected to a non-uniform magnetic field.

The M shape profile is thus present in many MHD pumps, a consequence of the position of the electrodes, and showing that different electrolytes solutions are similarly affected by this geometrical arrangement.

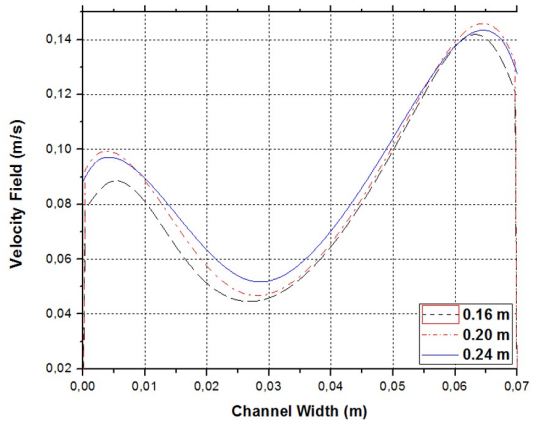

Figure 9. Fluid velocity profile along the *y*-axis for different *x* positions and 30 Volts.

The calculated current density along the channel is shown in figure 10 and can be obtained from the applied voltage. The current lines shown in figure 11 are also dependent on the applied voltage. To avoid the superposition of too many information, only the velocity pattern for 30 V is presented.

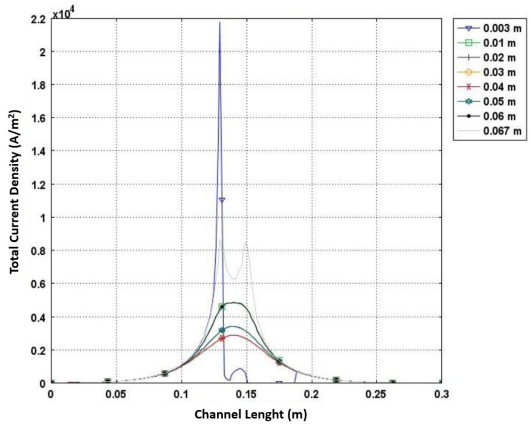

Figure 10. Total current density along the *x*-axis for different *y* positions and 30 volts.

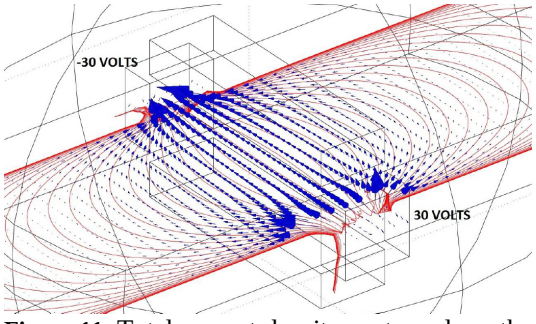

Figure 11. Total current density vectors along the *x*-axis for different *y* positions and 30 volts.

Using COMSOL, we still can plot the velocity and Lorentz force vector for easy viewing, according to figure 12 and 13.

Figures 12 and 13 present the velocity field and the Lorentz force field, respectively, allowing observing details close to the electrodes.

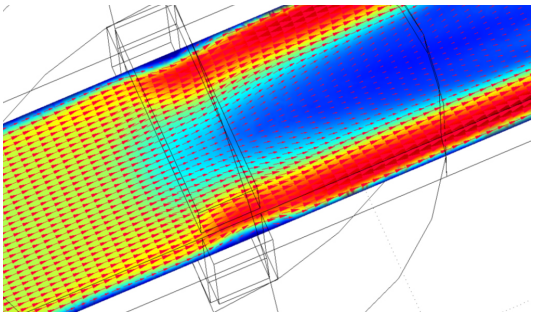

Figure 12. Velocity pattern along the channel for 30 volts.

In figures 12 and 13 the boundary conditions were set for straight channels (and not a closed circuit), for which no asymmetry is imposed. In this case, equal speeds are calculated in the left and right walls.

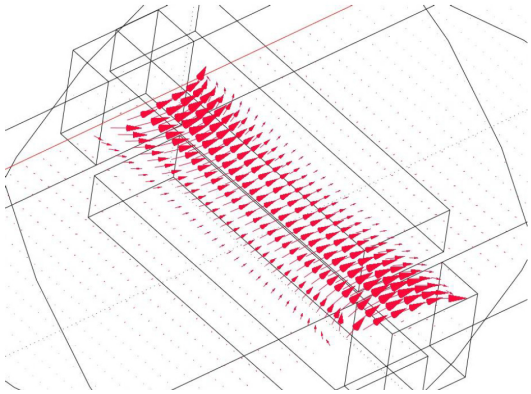

Figure 13. Lorentz force vectors along the channel for 30 volts.

Figure 12 shows an interesting aspect of the mass conservation condition in the channel flow. Upstream of the electrode, the imposed velocity is uniform. Downstream of the electrode, the fluid close to the walls was accelerated, implying in a deceleration of the fluid in the middle region of the channel. Of course, the M-shape of the velocity profile is the consequence of the conservation condition, as described, and the uneven distribution of the Lorentz force.

5. Conclusions

In this study, computational analyses were made to obtain results for an electromagnetic pump, considering a geometry already experimentally tested. The code COMSOL Multiphysics® 3.5a was used with the

options: k-ε turbulence model, magnetostatics, and conductive media. The DC models were able to solve the proposed flows, generating detailed profiles for different MHD parameters. An M-shaped profile was observed for the Lorentz force, as a consequence of the position of the electrodes. This M-shape was also observed in the velocity profiles, induced by the Lorentz forces. The velocities increase substantially with the voltage.

From the experimental information, the velocity profile is asymmetrical, a consequence of the closed circuit. This experimental information was inserted in the simulation through the boundary conditions

Considering a straight geometry, upstream of the electrode the imposed velocity was uniform. Downstream of the electrode the fluid close to the walls was accelerated, implying, from the mass conservation principle, in a deceleration of the fluid in the middle region of the channel. The M-shape of the velocity profile is, thus, the consequence of the mass conservation condition and the uneven distribution of the Lorentz force.

6. References

1. Ritchie, W., Experimental researches in a voltaic electricity and electromagnetism, *Philosophical transactions of the royal society of London*, **Vol**. **122**, pp. 279-298 (1832)
2. Williams, E. J., The induction of electromotive forces in a moving liquid by a magnet field, and its application to an investigation of the flow of liquids, *Proceedings of the physical society*, **Vol**. **45**, No. 5, pp. 466-478 (1930)
3. Kandev, N., Daoud, A., Magneto-hydrodynamic numerical study of DC electromagnetic pump for liquid metal, *Proceedings of the Comsol conference Hannover* (2008)
4. Andreev, O., Kolesnikov, Yu., Thess, A., Experimental study of liquid metal channel flow under the influence of a nonuniform magnetic field, *Physics of fluids*, **Vol. 18**, No. 6 (2006)
5. Ramos, I., Winowich, N. S., Finite difference and finite elements methods for MHD channel flows, *International journal for numerical methods in fluids*, **Vol. 11**, No. 6, pp. 907-934 (1990)
6. Lemoff, A. V., Lee, A. P., An AC magnetohydrodynamic micropump, *Sensors and actuators B:chemical*, **Vol. 63**, No. 3, pp. 178-185 (2000)
7. COMSOL Multiphysics., *Modeling guide*, Version 3.5a, pp. 1-518 (2008)
8. Kandev, N., Daoud, A., Electromagnetic DC pump of liquid aluminum: computer simulation and experimental study, *Fluid dynamics & materials processing*, **Vol. 224**, No. 1, pp. 1-28 (2009)